

Gene expression profiles of human proximal tubular epithelial cells in proteinuric nephropathies

M Rudnicki¹, S Eder¹, P Perco^{2,6}, J Enrich¹, K Scheiber³, C Koppelstätter¹, G Schratzberger¹, B Mayer⁴, R Oberbauer^{2,6}, TW Meyer⁵ and G Mayer¹

¹Division of Nephrology, Medical University Innsbruck, Innsbruck, Austria; ²Division of Nephrology, Medical University Vienna, Vienna, Austria; ³Department of Urology, Bezirkskrankenhaus Hall in Tirol, Hall in Tirol, Austria; ⁴Emergentec Biodevelopment GmbH, Vienna, Austria; ⁵Division of Nephrology, Stanford University School of Medicine, Stanford, California, USA and ⁶Department of Nephrology, KH Elisabethinen, Linz, Austria

In kidney disease renal proximal tubular epithelial cells (RPTEC) actively contribute to the progression of tubulointerstitial fibrosis by mediating both an inflammatory response and via epithelial-to-mesenchymal transition. Using laser capture microdissection we specifically isolated RPTEC from cryosections of the healthy parts of kidneys removed owing to renal cell carcinoma and from kidney biopsies from patients with proteinuric nephropathies. RNA was extracted and hybridized to complementary DNA microarrays after linear RNA amplification. Statistical analysis identified 168 unique genes with known gene ontology association, which separated patients from controls. Besides distinct alterations in signal-transduction pathways (e.g. Wnt signalling), functional annotation revealed a significant upregulation of genes involved in cell proliferation and cell cycle control (like insulin-like growth factor 1 or cell division cycle 34), cell differentiation (e.g. bone morphogenetic protein 7), immune response, intracellular transport and metabolism in RPTEC from patients. On the contrary we found differential expression of a number of genes responsible for cell adhesion (like BH-protocadherin) with a marked downregulation of most of these transcripts. In summary, our results obtained from RPTEC revealed a differential regulation of genes, which are likely to be involved in either pro-fibrotic or tubulo-protective mechanisms in proteinuric patients at an early stage of kidney disease.

Kidney International advance online publication, 20 December 2006;

doi:10.1038/sj.ki.5002043

KEYWORDS: proximal tubule; cell adhesion; gene expression; primary glomerulonephritis

Correspondence: M Rudnicki, Division of Nephrology, Medical University Innsbruck, Anichstrasse 35, 6020 Innsbruck, Austria
E-mail: michael.rudnicki@i-med.ac.at

Received 12 July 2006; revised 3 October 2006; accepted 1 November 2006

Usually end-stage renal failure is the terminal phase of a chronic disease and epidemiological studies indicate that up to 11% of the general population exhibit some abnormality of kidney function.^{1,2} Proteinuria has been accepted as a typical marker of kidney damage but urinary protein excretion has also been shown to actively contribute to the progression of the disease by affecting renal proximal tubular epithelial cell (RPTEC) function, and by promoting tubular atrophy and interstitial fibrosis. Increased glomerular filtration has been described for many potentially tubulotoxic proteins: *In vitro* albumin stimulates the expression of monocyte chemoattractant protein-1 and interleukin-8 via reactive oxygen species generation^{3,4} and in an animal model of proteinuric renal disease blockade of monocyte chemoattractant protein-1 expression attenuates tubulointerstitial injury.⁵ When incubated with delipidated albumin, immunoglobulin G, or transferrin, RPTEC show increased expression of endothelin-1, which represents a strong chemoattractant for monocytes and macrophages.⁶ Similarly the production of regulated upon activation normal T-cell expressed and secreted and transforming growth factor-beta1 (TGF- β 1)^{7,8} is increased and the expression of insulin-like growth factor-1 (IGF-1) is altered.⁹ Thus, in RPTEC proteinuria induces a gene expression profile, which favors the recruitment of macrophages and promotes tubular atrophy and interstitial fibrosis. In the last decade the epithelial-to-mesenchymal transition (EMT) of tubule cells has been identified as another significant mechanism, which contributes to progression of tubulointerstitial fibrosis. Factors with the ability to induce EMT include TGF- β 1, epidermal growth factor, basic fibroblast growth factor, and interleukin-1.¹⁰ Just recently bone morphogenetic protein 7 (BMP-7) has been found to counteract TGF- β 1 induced EMT and to reverse chronic renal injury.¹¹ However, it is not clear if human RPTEC display changes of global gene expression at early stages of proteinuric kidney disease when excretory renal function is close to normal. The objective of this study was, therefore, to identify genes and pathways specifically in human RPTEC using complementary (cDNA) microarrays. Normal renal tissue sections obtained from the unaffected

part of organs removed because of renal cell carcinoma served as controls.

RESULTS

Microarray quality

All microarray experiments were processed as technical duplicates. Average Pearson's correlation coefficient between two replicate arrays was 0.95. We used the sector analysis of variance tool from the Stanford Microarray Database to check every single microarray for hybridization artefacts.¹² The mean r^2 sector analysis of variance value of 0.019 ± 0.015 indicated no evidence of a hybridization bias.

Genes, biological processes, and pathways expressed differentially between proteinuric patients and control subjects

A supervised cluster analysis using significance analysis of microarrays and a *t*-test with max *t*-correction for multiple testing in order to identify subsets of genes differentially regulated between proteinuric patients and healthy controls reported 261 (significance analysis of microarrays) and 58 (*t*-test) differentially regulated cDNA clones. A combination of both methods resulted in 275 cDNA clones representing 230 unique genes, 168 of which could be assigned to gene ontology terms (Table 1); the remaining 62 sequences were hypothetical proteins, open-reading frames, and expressed sequence tags (Table S1). The ratio of up- and downregulated genes was balanced with 83 of the 168 genes being significantly up- and 85 genes being downregulated in proteinuric patients. The complete list of enriched PANTHER ontology categories (i.e. biological processes which are found to show a higher or a lower prevalence in patients than in a reference gene list) is shown in Tables S2 and S3.

Apoptosis. We found a decreased expression of the BCL-2-interacting killer and the human T-cell leukemia virus type 1 binding protein 1. Although BCL-2-interacting killer is known to facilitate programmed cell death via interaction with survival-promoting proteins (e.g. *bcl2*), T-cell leukemia virus type 1 binding protein 1 exerts antiapoptotic properties. TIA1 cytotoxic granule-associated RNA binding protein was also downregulated, however its exact role in apoptosis is unclear.

Cell adhesion and differentiation. Significant alterations in the expression of the cell adhesion genes thrombospondin-3 (TSP-3, THBS3), a disintegrin and metalloproteinase domain 22, neural cell adhesion molecule 1, contactin 3, BH-protocadherin7, CD226 antigen, fibronectin 1, collagen type 16 alpha 1 and cysteine-rich angiogenic inducer 61 suggest proteinuria induced decrease in cell-to-cell and cell-to-matrix interactions of RPTEC. TSP-3, a recently discovered member of the TSP family with a functional role in cell adhesion,¹³ shares a sequence similarity in the COOH terminus with TSP-1. The balance between the latter and fibronectin, whose expression was also changed, has recently been proposed as an early indicator of aberrant proximal tubule and collecting duct differentiation.¹⁴

We did not find significant differential expression of TGF- β 1 – the most prominent inducer of EMT. However, we observed a downregulation of V-ski sarcoma viral oncogene homolog (SKI). Reduced expression of ski has been described in fibrotic kidney after obstructive injury, and it has been shown that the loss of ski expression *in vitro* might amplify TGF- β 1 signalling.¹⁵ On the other hand the expression of BMP-7 was strongly and consistently elevated in proteinuric subjects.

Interestingly we also found a reduced expression of cysteine-rich angiogenic inducer 61. Cysteine-rich angiogenic inducer 61 is a growth factor-inducible protein responsible for promotion of cell proliferation as well as of cell adhesion through the interaction with integrins. The marked downregulation of this transcript is compatible with a decreased cell adhesion but also links proteinuria to an inhibition of fibroblast apoptosis, as very recently suggested by Todorovic *et al.*¹⁶

Cell proliferation and cell cycle control. Increased expression of IGF-1 as well as of cell division cycle 34, annexin 13, ras-related oncogene and mitogen-activated protein (MAP)/microtubule affinity-regulating kinase 3 – which is a CDC25C associated protein promoting the cell cycle at G2/M transition – points to an enhanced proliferation of RPTEC. This hypothesis is further underlined by decreased expression of three phosphatases, which negatively regulate cell growth, namely the magnesium-dependent protein phosphatases 1D and 1B and the phosphatidic acid phosphatase type 2A. These findings underscore recent *in vitro* results showing that albumin – at least at low concentrations and with a high fatty acid content – stimulates cell turn-over by stimulating proliferation of tubule cells.^{17–19}

Immune response. We found a modulated expression of several genes involved in immune response: Defensin beta 1 (DEFB1), interferon gamma receptor 1, the q subcomponent of the receptor of complement component 1, stress-associated endoplasmic reticulum protein 1 and tyrosyl-protein sulfotransferase were strongly upregulated. The expression of C-associated protein of tyrosine phosphatase (a protein associated with CD45), chemokine (C-C) ligand 5, the natural killer recognition sequence, colony stimulating factor 1 and calcium modulating ligand was diminished.

Transport, metabolism, and matrix turnover. Not surprisingly several genes responsible for intracellular transport and amino-acid/protein metabolism were activated in proteinuric patients as were genes involved in degradation of proteins (ubiquitin-conjugating enzyme E2L 6, ubiquitin-like 4, ubiquitin-conjugating enzyme E2M, ubiquitin-activating enzyme E1C, F-box and WD-40 domain protein 4 and F-box and leucine-rich repeat protein 7).

Expression of nine genes involved in lipid metabolism was altered in our experiments with a predominant upregulation in patients. Four of these are known to participate in several steps of fatty acid degradation, that is, dehydrogenase/reductase (SDR family) member 3, branched chain acyl-coenzyme A oxidase 2, palmitoyl acyl-coenzyme A oxidase 1

Table 1 | Functional characterization of 168 genes differentially regulated between patients and controls utilizing GO-terms

Accession number	Gene name	Symbol		Fold change
<i>Apoptosis</i>				
AI347538	BCL2-interacting killer (apoptosis inducing)	BIK	–	2.23
R33840	TIA1 cytotoxic granule-associated RNA binding protein	TIA1	–	2.14
W84733	Tax1 (human T-cell leukemia virus type I) binding protein 1	TAX1BP1	–	1.91
<i>Cell adhesion</i>				
AA774044	Thrombospondin 3	THBS3	+	3.67
N29801	A disintegrin and metalloproteinase domain 22	ADAM22	+	2.41
AI214500	Neural cell adhesion molecule 1	NCAM1	–	2.89
N50845	Contactin 3	CNTN3	–	2.59
AA428239	BH-protocadherin	PCDH7	–	2.47
AI361991	CD226 antigen	CD226	–	2.56
AA953560	Fibronectin 1	FN1	–	2.47
AA088202	Collagen, type XVI, and alpha 1	COL16A1	–	2.16
AI014487	Cysteine-rich, angiogenic inducer, 61	CYR61	–	3.66
<i>Cell proliferation/cell-cycle control</i>				
AA456321	Insulin-like growth factor 1 (somatomedin C)	IGF1	+	2.67
H20742	Cell division cycle 34	CDC34	+	2.73
AI984289	Annexin A13	ANXA13	+	3.47
AI368184	Related RAS viral (r-ras) oncogene homolog	RRAS	+	1.80
H09721	MAP/microtubule affinity-regulating kinase 3	MARK3	+	2.14
AI024631	Protein phosphatase 1D	PPM1D	–	2.25
AW028938	Protein phosphatase 1B	PPM1B	–	2.88
AA598865	Phosphatidic acid phosphatase type 2A	PPAP2A	–	2.88
<i>Cell differentiation</i>				
AI886264	Bone morphogenetic protein 7 (osteogenic protein 1)	BMP7	+	4.18
H92070	V-ski sarcoma viral oncogene homolog (avian)	SKI	–	2.23
<i>Immune response</i>				
AA946653	Defensin, beta 1	DEFB1	+	7.67
H11482	Interferon gamma receptor 1	IFNGR1	+	2.98
AA150505	Complement component 1, q subcomponent, and receptor 1	C1QR1	+	2.42
AA172210	Stress-associated endoplasmic reticulum protein 1	SERP1	+	2.63
N52474	Tyrosylprotein sulfotransferase 1	TPST1	+	2.97
AA481547	Protein tyrosine phosphatase, receptor type, and C-associated protein	PTPRCAP	–	3.62
AA873792	Chemokine (C-C motif) ligand 5	CCL5	–	2.47
AI382982	Natural killer-tumor recognition sequence	NKTR	–	2.16
AI242464	Colony stimulating factor 1 (macrophage)	CSF1	–	2.09
R14080	Calcium modulating ligand	CAMLG	–	2.39
<i>Transport (intracellular)</i>				
H93459	RAB4A, member RAS oncogene family	RAB4A	+	7.96
AA155803	RAB43, member RAS oncogene family	RAB43	+	2.70
AA169814	Sorting nexin 2	SNX2	+	3.34
AA917609	SEC6-like 1	SEC6L1	+	2.77
R55992	SEC14-like 1	SEC14L1	+	2.85
AA069704	Translocase of outer mitochondrial membrane 7 homolog	TOMM7	+	2.58
AA972020	RAB6 interacting protein 2	RAB6IP2	–	2.72
AI272812	Mitochondrial carrier triple repeat 6	MCART6	–	2.36
AA284180	EH-domain containing 1	EHD1	–	1.98
<i>Transport (membrane)</i>				
AA155640	Transcobalamin I (vitamin B12 binding protein, R binder family)	TCN1	+	3.97
AA626279	Potassium voltage-gated channel, Shal-related subfamily, member 3	KCND3	+	1.97
AI075049	Aquaporin 2 (collecting duct)	AQP2	+	6.14
H09087	Aquaporin 4	AQP4	+	2.29
H23170	Solute carrier family 1 (high-affinity aspartate/glutamate transporter), member 6	SLC1A6	–	1.99
AA166885	Solute carrier family 12, (potassium-chloride transporter) member 5	SLC12A5	–	2.26
W01500	Transient receptor potential cation channel, subfamily C, member 1	TRPC1	–	3.65
H69810	Chloride channel 3	CLCN3	–	2.71
<i>Metabolism (amino acid and protein)</i>				
R10382	Serine (or cysteine) proteinase inhibitor, member 5 (=protein C inhibitor)	SERPINA5	+	8.05
AW071596	Ubiquitin-conjugating enzyme E2L 6	UBE2L6	+	3.26
N64628	Ubiquitin-like 4	UBL4	+	2.64

Table 1 | Continued

Accession number	Gene name	Symbol		Fold change
AI971344	Ubiquitin-conjugating enzyme E2M (UBC12 homolog, yeast)	UBE2M	+	2.42
AI309770	Ubiquitin-activating enzyme E1C (UBA3 homolog, yeast)	UBE1C	+	1.92
AA463476	F-box and WD-40 domain protein 4	SHFM3	+	3.26
AA630881	F-box and leucine-rich repeat protein 7	FBXL7	+	2.78
R52639	Serine hydroxymethyltransferase 1 (soluble)	SHMT1	+	3.17
AA733022	FK506 binding protein 14, 22 kDa	FKBP14	+	2.85
AA481353	Branched chain aminotransferase 2, mitochondrial	BCAT2	+	2.69
AA676588	Chaperonin containing TCP1, subunit 7 (eta)	CCT7	+	2.49
AI923312	Calpain 6	CAPN6	+	2.39
AA664056	Prolyl endopeptidase	PREP	–	2.46
T95267	DnaJ (Hsp40) homolog, subfamily C, member 12	DNAJC12	–	2.77
H80214	Tissue inhibitor of metalloproteinase 1	TIMP1	–	5.11
<i>Metabolism (lipid)</i>				
AA160106	Acid phosphatase 6, lysophosphatidic	ACP6	+	3.00
AA211446	1-acylglycerol-3-phosphate O-acyltransferase 3	AGPAT3	+	3.54
W95082	Hydroxysteroid (11-beta) dehydrogenase 2	HSD11B2	+	3.14
AA171606	Dehydrogenase/reductase (SDR family) member 3	DHRS3	+	3.08
R25823	Acetyl-coenzyme A acetyltransferase 2 (acetoacetyl coenzyme A thiolase)	ACAT2	+	2.18
T71713	Acyl-coenzyme A oxidase 2, branched chain	ACOX2	+	2.62
T62985	Acyl-coenzyme A oxidase 1, palmitoyl	ACOX1	–	2.60
H95792	Acyl-coenzyme A dehydrogenase, short/branched chain	ACADSB	–	2.49
AA481034	Copine 1	CPNE1	–	2.43
<i>Metabolism (carbohydrate)</i>				
AA157261	Phosphatidylinositol glycan, class Q	PIGQ	+	3.41
AA609458	ST6 beta-galactosamide alpha-2,6-sialyltransferase 2	SIAT2	+	3.34
AW087924	Aldolase A, fructose-bisphosphate	ALDOA	+	2.57
AW002307	Malic enzyme 1, NADP(+)-dependent, cytosolic	ME1	–	3.31
AI652382	TDP-glucose 4,6-dehydratase	TGDS	–	2.37
AI216166	UDP-Gal:betaGlcNAc beta 1,3-galactosyltransferase, polypeptide 4	B3GALT4	–	2.31
<i>Metabolism (nucleic acids)</i>				
AI961991	Poly(A)-specific ribonuclease (deadenylation nuclease)	PARN	–	2.09
AA598487	Phosphoribosylglycinamide formyltransferase	GART	–	2.26
<i>Metabolism (general)</i>				
T39503	Epoxide hydrolase 1, microsomal (xenobiotic)	EPHX1	+	3.14
AA401241	E-1 enzyme	MASA	+	2.88
AA436549	Nitric oxide synthase interacting protein	NOSIP	+	2.12
AA884967	Nitric oxide synthase 3 (endothelial cell)	NOS3	–	2.16
AA417700	PH domain and leucine-rich repeat protein phosphatase-like	KIAA0931	–	2.41
AI262683	N-acetyltransferase 2 (arylamine N-acetyltransferase)	NAT2	–	2.23
AI081368	Adenylate cyclase 1 (brain)	ADCY1	–	1.65
<i>Signal transduction</i>				
R06605	Protein tyrosine phosphatase, non-receptor type 1	PTPN1	+	5.55
N79051	V-ros UR2 sarcoma virus oncogene homolog 1 (avian)	ROS1	+	2.83
AA463213	Protein kinase D3	PRKD3	+	2.09
AA171899	Butyrate-induced transcript 1	HSPC121	+	4.56
AW087914	Casein kinase 1, delta	CSNK1D	+	2.82
AA992441	COP9 constitutive photomorphogenic homolog subunit 6 (<i>Arabidopsis</i>)	COPS6	+	2.76
AI146565	Neuromedin U	NMU	+	2.27
AW044654	Frequently rearranged in advanced T-cell lymphomas	FRAT1	+	1.96
R36143	Glutamate receptor interacting protein 1	GRIP1	–	3.69
AA461086	Phosphodiesterase 5A, cGMP-specific	PDE5A	–	3.69
T67004	Endothelin 3	EDN3	–	3.37
R20227	Guanine nucleotide binding protein (G protein)	GNAO1	–	2.99
W65460	Dual specificity phosphatase 5	DUSP5	–	2.96
H97140	Dual specificity phosphatase 8	DUSP8	–	2.41
AA699578	Casein kinase 1, alpha 1	CSNK1A1	–	2.42
AA130874	Protein tyrosine phosphatase, non-receptor type 14	PTPN14	–	2.31
H63668	Casein kinase 2, alpha prime polypeptide	CSNK2A2	–	2.26
AI267935	RAB26, member RAS oncogene family	RAB26	–	2.06
AA678971	Regulator of G-protein signalling 9	RGS9	–	1.82
AA496519	Transducin-like enhancer of split 3 (E(sp1) homolog, <i>Drosophila</i>)	TLE3	–	1.74
AI274270	Alpha-kinase 1	ALPK1	–	3.60

Table 1 | Continued

Accession number	Gene name	Symbol		Fold change
N34513	Doublecortin and CaM kinase-like 1	DCAMKL1	–	2.59
H51569	CaM kinase-like vesicle-associated	MGC8407	–	2.18
AA670373	Protein phosphatase 1, regulatory (inhibitor) subunit 14C	PPP1R14C	–	1.86
AA481277	Rho guanine nucleotide exchange factor (GEF) 1	ARHGEF1	–	2.60
<i>Structural</i>				
AA083485	Ribosomal protein L19	RPL19	+	5.95
AA774983	Tropomyosin 4	TPM4	+	2.98
AW078724	Tubulin, beta, 2	TUBB2	+	2.97
H23421	Ribosomal protein L7a	RPL7A	+	2.83
AA486224	Syncoilin, intermediate filament 1	SYNCOILIN	+	2.76
AA426081	Ribosomal protein S14	RPS14	+	2.62
T71680	Mitochondrial ribosomal protein L30	MRPL30	+	2.40
AA211796	SMC2 structural maintenance of chromosomes 2-like 1 (yeast)	SMC2L1	+	1.95
H93604	Formin binding protein 1	FNBP1	–	2.45
AI038302	Matrilin 4	MATN4	–	2.23
AA464952	Gamma tubulin ring complex protein (76p gene)	76P	–	2.23
AA404360	SMC5 structural maintenance of chromosomes 5-like 1 (yeast)	SMC5L1	–	2.19
<i>Transcription/translation</i>				
AA157011	MADP-1 protein	MADP-1	+	2.96
AW087156	PWP1 homolog (<i>S. cerevisiae</i>) 'endonuclease'	PWP1	+	4.35
W31688	Sp3 transcription factor	SP3	+	4.28
AA088434	Zinc-finger protein 3 (A8-51)	ZNF3	+	3.99
AA620571	Small nuclear RNA activating complex, polypeptide 3, 50 kDa	SNAPC3	+	3.59
AW087153	Mortality factor 4 like 2	MORF4L2	+	3.39
T62072	YEATS domain containing 4	YEATS4	+	2.66
AA485991	Transcription factor CP2	TFCP2	+	2.57
AA025648	Hairless homolog (mouse)	HR	+	2.56
AA419164	Retinoic acid receptor, beta	RARB	+	2.46
R56552	Forkhead box K2	FOXP2	+	2.44
N47961	GLIS family zinc finger 1	GLIS1	+	2.39
AA478656	General transcription factor IIF, polypeptide 2, 30 kDa	GTF2F2	–	3.82
AA928017	POU domain, class 2, associating factor 1	POU2AF1	–	3.06
AA446027	Early growth response 2 (Krox-20 homolog, <i>Drosophila</i>)	EGR2	–	2.80
AI218732	Nuclear receptor subfamily 2, group C, member 2	NR2C2	–	2.57
R10443	Zinc-finger protein, subfamily 1A, 5	ZNFN1A5	–	2.53
H97146	ELK3, ETS-domain protein (SRF accessory protein 2)	ELK3	–	2.53
AA206370	RNA binding motif protein 15	RBM15	–	2.38
N49703	Chromodomain helicase DNA binding protein 2	CHD2	–	2.30
H38771	Myeloid/lymphoid or mixed-lineage leukemia 5 (trithorax homolog, <i>Drosophila</i>)	MLL5	–	2.27
AA484950	Vitamin D (1,25- dihydroxyvitamin D3) receptor	VDR	–	2.18
AI214272	Forkhead box J3	FOXJ3	–	2.13
N72495	Zinc-finger homeodomain 4	ZFH4	–	2.01
N66572	Spleen focus forming virus (SFFV) proviral integration oncogene spi1	SPI1	–	1.76
AA482389	Zinc-finger protein 292	ZNF292	–	1.59
AI368766	Eukaryotic translation elongation factor 1 alpha 2	EEF1A2	–	2.33
AA233901	KIAA0863 protein	KIAA0863	–	2.25
<i>Hemostasis</i>				
T67549	Plasminogen-like B1	PLGL	+	6.81
N98524	Coagulation factor X	F10	–	2.26
<i>Hormone binding</i>				
T69271	Sex hormone-binding globulin	SHBG	+	3.84
<i>Nucleus</i>				
H15111	Uracil-DNA glycosylase	UNG	+	4.70
T59256	Prickle-like 2 (<i>Drosophila</i>)	PRICKLE2	+	3.07
AA953294	Sjogren's syndrome nuclear autoantigen 1	SSNA1	+	2.72
AI888464	Cleavage stimulation factor, 3' pre-RNA, subunit 1, 50 kDa	CSTF1	+	2.37
AA398090	Nucleoporin like 2	NUPL2	–	3.20
AA417948	TRNA selenocysteine-associated protein	SECP43	–	2.44
<i>Membrane</i>				
W47484	Opioid receptor, sigma 1	OPRS1	+	3.53
AA126879	Mal, T-cell differentiation protein 2	MAL2	+	2.93

Table 1 | Continued

Accession number	Gene name	Symbol		Fold change
N26125	Neuropilin 2	NRP2	–	2.51
R71781	EPS8-like 1	EPS8L1	–	2.23
AA047567	Progesterone receptor membrane component 2	PGRMC2	–	2.18
AA453486	Signal sequence receptor, gamma (translocon-associated protein gamma)	SSR3	–	2.43

Numbers are fold changes. (+) indicates upregulation in patients, whereas (–) indicates suppressed sequences.

and short/branched chain acyl-coenzyme A dehydrogenase. We also found a strong upregulation of the expression of hydroxysteroid (11-beta) dehydrogenase 2, an enzyme that catalyzes the conversion of cortisol to the inactive metabolite cortisone.

We found differentially regulated expression of proteinase-inhibitors: although the expression of serine proteinase inhibitor 5 was markedly increased, the expression of tissue inhibitor of metalloproteinase 1 (collagenase 1; TIMP1) was reduced. Serine proteinase inhibitor 5, also known as protein C inhibitor or plasminogen activator inhibitor 3 is synthesized and localized in kidney tissue where it provides unspecific protease inhibitory activity.²⁰ Interestingly, *in vitro* experiments with plasminogen activator inhibitor 1 and plasminogen activator inhibitor 3 in breast cancer cell lines suggest a downstream effect of these proteins on the expression of cell adhesion molecules of the integrin family.²¹

TIMP1 modulates extra-cellular matrix turnover by inhibition of several members of the metalloproteinase family. Just recently it was shown that hepatocyte growth factor – known for its antifibrotic effects – reduced the expression of TGF- β 1, collagen IV alpha 2, TIMP-1, and increased metalloproteinase-2 levels in glomerular cells of donor kidney biopsies²² suggesting an interesting multiway relationship between hepatocyte growth factor, TGF- β 1, TIMP-1 and metalloproteinases.

In addition to changes in carbohydrate and nucleic acid metabolism alterations in two other metabolic transcripts seem worth mentioning: nitric oxide synthase interacting protein and nitric oxide synthase 3 (NOS3 = eNOS; i.e. endothelial isoform of NOS). Proteinuria caused a strong upregulation of nitric oxide synthase interacting protein and a reduced expression of NOS3. Recently, eNOS has been identified as the NOS isoform responsible for NO production and regulation of NaCl absorption by the thick ascending loop of Henle.²³ This effect seems to be regulated by luminal flow. However, the role of eNOS in the proximal tubule cell is more controversial and still not elucidated.²⁴ Interestingly, nitric oxide synthase interacting protein has been proposed as a modulator of eNOS activity, but its expression in renal tubule cells has not been described yet.²⁵

Signal transduction. We found differential expression of several transcripts involved in the Wnt-signalling pathway (casein kinase 1: delta and alpha 1, FRAT1, alpha prime polypeptide of casein kinase 2 and TLE3). Furthermore the expression of non-receptor type 1 protein tyrosine phosphatase (PTPase, PTPN1), which has been shown to be a negative regulator of insulin- and IGF-1-stimulated signalling, was increased. On the other hand the expression of another PTPase, the non-receptor type 14 PTPase, was reduced. Two members of the dual specificity phosphatase superfamily dual specificity phosphatase 5 (DUSP5) and DUSP8 showed a decreased expression. These phosphatases negatively regulate members of the MAP kinase superfamily, which are associated with cellular proliferation and differentiation. DUSP5 has a substrate specificity towards the extracellular signal-regulated kinase (ERK) family of MAP kinases, whereas DUSP8 predominantly inactivates stress-activated protein kinase/c-Jun N-terminal kinase and p38.

Transcription factors. Among all the genes differentially expressed between patients and controls we found 12 transcription factors up- and 16 downregulated in the patient group. Five of the 12 upregulated transcription factors have previously been implicated in the regulation of growth, cell proliferation and cell differentiation (PWP1, ZNF3, mortality factor 4-like protein 2, YEATS4 and RARB). Both mortality factor 4-like protein 2 and YEATS4 encode components of the *nua4* histone acetyltransferase complex which is involved in the activation of transcriptional programs associated with oncogene growth-induction, tumor suppressor mediated growth arrest and replicative senescence, apoptosis and DNA repair. In the group of downregulated transcription factors we found – among others – decreased expression of early growth response-2 and ELK3 transcription factors. Early growth response family members (in particular early growth response-2 and early growth response-3) regulate nonlymphoid expression of Fas ligand, tumor necrosis factor-related apoptosis-inducing ligand, and tumor necrosis factor during immune response and may induce apoptosis of T cells.²⁶ ELK-3 is a member of the ternary complex factors subfamily of Ets proteins, along with ELK-1 and Sap-1, which are involved in transcriptional regulation of genes important for determining tissue specificity, cellular differentiation, and cellular proliferation.

Real-time PCR analysis of selected genes

We selected five genes from five different functional groups for validation experiments by Taqman real-time polymerase chain reaction (PCR) analysis, namely DEFB1, TIMP1, DUSP5, BMP7, and RAB4A. We used glyceraldehyde-3-phosphate dehydrogenase (GAPDH) as the endogenous control. A high correlation between array and real-time

PCR results was observed for all five genes (Figure 1). In particular, there were no directional changes, and the Pearson correlation between array and PCR was 0.79–0.81.

Immunohistochemical localization of TSP-3 and BMP-7 in kidney biopsies

We selected two proteins from two functional groups to underscore our gene expression results: TSP-3 (cell adhesion) and BMP-7 (cell differentiation). Conventional immunohistochemistry showed a low expression of TSP-3 in nearly all tubules in control samples (Figure 2a) and a significant increase of expression in patients (Figure 2b). The immunohistochemical staining showed no BMP-7 expression in control subjects except in distal tubules (Figure 3a). However, in proteinuric patients we saw a strong expression of this protein in nearly all tubules (Figure 3b). Interestingly, we found the strongest immunohistochemical signal of BMP-7

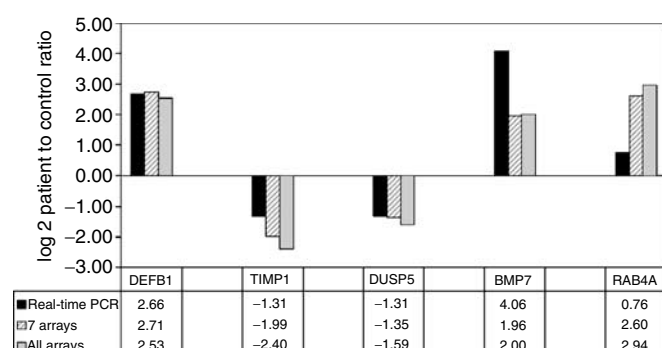


Figure 1 | Taqman real-time PCR analysis of five selected genes from Table 1. DEFB1 (Hs.32949), TIMP1 (Hs.522632), DUSP5 (Hs.2128), BMP7 (Hs.473163) and RAB4A (member of the *ras* oncogene family, Hs.296169). All numbers represent log-transformed fold-change values between patients and controls where positive values indicate higher expression in patients. The real-time PCR results were calculated as relative expression to the internal standard glyceraldehyde-3-phosphate dehydrogenase using the delta-delta-ct method. Real-time experiments showed a Pearson's correlation of 0.81 when compared to Microarray results of the seven selected patients, and 0.79 when compared to expression values from all patients, respectively (see Materials and Methods section).

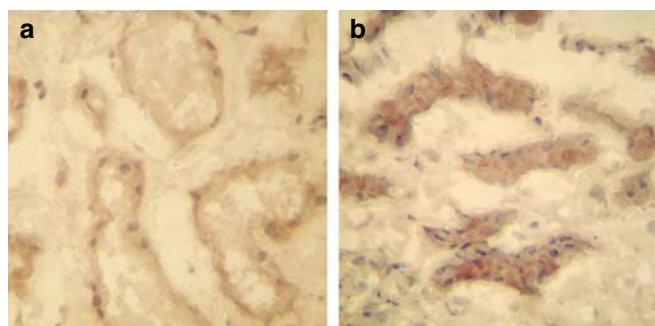


Figure 2 | Immunohistochemical staining of TSP-3. (a, b) Immunostaining for TSP-3: original magnification $\times 40$. (a) In control subjects we found a weak TSP-3 signal in all tubule cells. (b) In proteinuric patients a strong positive staining for TSP-3 was observed in most of the tubule cells.

protein at the luminal side of tubular epithelial cells. Neither of those proteins was detected in the glomeruli.

DISCUSSION

In this study we combined two innovative, novel and potent technologies: We isolated specifically RPTEC from patients and controls using laser capture microdissection, and we performed transcriptome analysis using cDNA microarray technology. This approach has several striking advantages: (a) our results can clearly be attributed to RPTEC, which have been shown to be a key player in the pathogenesis of progressive renal disease. (b) Genome-wide gene expression analysis and bioinformatic workup is the only way to identify regulatory networks affected by proteinuria overcoming many shortfalls of 'single-gene' approaches. (c) Using human biopsies the problems of interpretation of animal and/or cell culture can be avoided.

Supervised analysis showed significant transcriptional differences in genes, which play a major role in cell adhesion, cell proliferation, cell cycle control, cell differentiation, and in lipid-, amino-acid-, and protein-metabolism as well as in the groups of intracellular- and membrane-transport protein coding genes.

The differential regulation of genes involved in intracellular transport, amino-acid-, and protein- as well as lipid-metabolism reflects enhanced reabsorption and degradation of proteins via ubiquitination in the state of proteinuria. It has been demonstrated *in vitro* in opossum kidney cells²⁷ and in human proximal tubular cells¹⁷ as well as *in vivo* in a murine animal model¹⁸ that proteinuria – notably albuminuria – is linked with proliferation of tubular cells. Dixon and Brunskill²⁷ showed that albumin-induced stimulation of growth and proliferation of proximal tubular cells is dependent on the ERK family of MAP kinases, whose activity is also likely to be increased in our patients owing to the reduced activity of DUSP5 and DUSP8. The findings of Takaya *et al.*²⁸ suggest an involvement of the ERK pathway in BSA-induced monocyte chemoattractant protein-1 expression in mouse proximal tubular cells, and the authors suggest

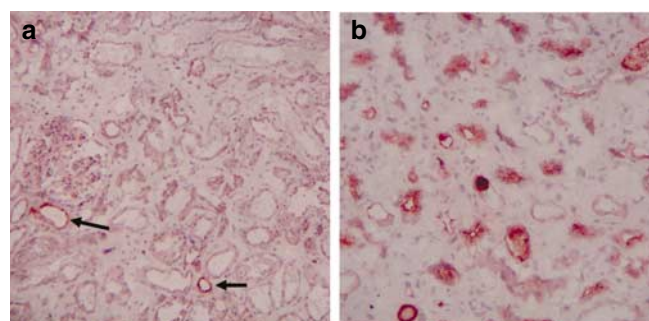


Figure 3 | Immunohistochemical staining of BMP-7. (a, b) Immunostaining for BMP-7: original magnification $\times 20$. (a) In healthy subjects we did not detect any positive BMP-7 signal in proximal tubules and neither in the glomeruli. Arrows: there are single distal tubules with a weak BMP-7 staining. (b) Stable proteinuric patients showed a strong BMP-7 staining in tubule cells. Interestingly, we found the most prominent staining at the luminal side of the cells.

as well a possible interaction of nuclear factor-kappaB with ERK. Accordingly, we observed a significant transcriptional change in the functional category of immune response genes. We also found an elevated expression of IGF-1 in proteinuric patients. IGF-1 has been studied extensively in the context of hypertrophic renal growth associated with common renal diseases like diabetic nephropathy. In murine tubular epithelial cells IGF-1 stimulates the activities of the MAP kinases ERK1/ERK2.²⁹ These findings strongly indicate a proliferative state in human RPTEC exposed to proteinuria, at least at an early stage of disease.

The role of apoptosis of tubular cells in the pathogenesis of progressive renal disease is still discussed controversially.³⁰ On the one hand it was shown in numerous studies that albumin induces apoptosis of proximal tubule cells,^{31,32} on the other hand Iglesias *et al.*³³ showed that albumin is a major survival factor for tubule cells through scavenging of reactive oxygen species. Considering the simultaneous decreased expression of pro- and antiapoptotic stimuli and the lack of significant transcriptional alterations of well-characterized apoptosis-related genes, we cannot draw a definitive conclusion with respect to the impact of programmed cell death at this stage of disease.

Our analysis identified a significant downregulation of genes involved in cell adhesion in RPTEC from patients, compatible with the induction of EMT. An emerging body of evidence suggests numerous signalling pathways as initiators of EMT of proximal tubular cells, the final common hallmark being a decrease in E-cadherin expression, resulting in reduced cell-cell interaction and diminished adhesion of tubule cells to the basolateral membrane.¹⁰ EMT is an important process which enables tubular epithelial cells to acquire a mesenchymal phenotype, migrate from the tubular lumen into the interstitium and escape apoptosis. TGF- β 1 has been described as one of the main inducers of EMT. However, EMT would ultimately lead to a loss of organ function and therefore counter-regulatory pathways are present. It has been suggested that finally an imbalance between pro- and antifibrotic growth factors/hormones determines the fate of the kidney.^{34,35} In our patients renal function was well maintained and tubulointerstitial fibrosis was minimal despite a mean duration of the disease of 7 months before biopsy. Furthermore, serum creatinine values were stable during a follow-up period of 2 years. However, one has to acknowledge that some patients received immunosuppressive therapy after the biopsy. Nonetheless, at least at the time of biopsy protective mechanisms might sufficiently counteract the above-described deleterious effects. One of the endogenous antagonists of TGF- β 1 with respect to EMT is bone morphogenic protein-7 (BMP-7). BMP-7 expression was significantly elevated in our patient samples, and we confirmed the results as well on the protein level. Our findings are compatible with the data obtained by Zeisberg *et al.*¹¹ who showed *in vitro* that chronic renal injury induced by TGF- β 1 can be counteracted and even reversed by the application of BMP-7, suggesting an association of those

two molecules within the intracellular pathways. In many animal models of chronic kidney injury these results were confirmed unequivocally showing that administration of BMP-7 has positive therapeutic effects in terms of reduced injury, accelerated regeneration, inhibition of tubular atrophy, inhibition of interstitial fibrosis, and even improvement of glomerular filtration rate.^{11,36-40}

In addition, the differential regulation of genes involved in Wnt signalling is in line with the idea of simultaneous presence of proteinuria associated injury and repair mechanisms. Just recently, the Wnt signalling system has been implicated as a new potential mediator of mesenchymal-to-epithelial transition in murine models of acute renal failure⁴¹ and unilateral urethral obstruction.⁴² The key factor of Wnt signalling is β -catenin. The intracellular-concentration of β -catenin, which is regulated by degradation of β -catenin by paired phosphorylation through the serine/threonine kinases casein kinase I and glycogen synthase-3 β is the rate determining factor of the Wnt-signalling cascade. Interestingly, recent studies showed several connections between Wnt- and β -catenin signalling and cadherin-mediated cell adhesion, in which also the key event is β -catenin stability and availability.⁴³ In our experiments we found a differential expression of three isoforms of casein kinase I: delta (upregulated), alpha 1, and alpha prime polypeptide (down-regulated). Furthermore, we found two PTPases to be as well differentially regulated between patients and controls: PTPN1 (up) and PTPN14 (down). Activation of PTPases has been implicated in the stabilization of the cadherin-catenin complex resulting in increased cadherin-mediated cell-cell adhesion.⁴⁴ Although we did not find a differential expression of the main members of the Wnt-gene family (e.g. Wnt-4), the significant accumulation of these kinases and phosphatases suggests a well-balanced regulation of the cadherin-catenin complex in human RPTEC exposed to proteinuria.

Our study has several limitations, the major probably being the limited number of samples being included. As we used a very stringent statistical analysis it is likely that this fact might have precluded the identification of additional, potentially at least as important genetic alterations. Furthermore, we monitored changes in transcriptional profiles, and it is unclear if indeed identical profiles would be obtained on a protein level, despite encouraging immunostaining results for two of these genes. This might especially hold true for several well known key mediators in the pathogenesis of renal fibrosis, for example, TGF- β 1, monocyte chemoattractant protein-1, ET-1, regulated upon activation normal T-cell expressed and secreted, platelet-derived growth factor-AB, and interleukin-8 as well as nuclear factor NF-kappaB and others, where we did not see any significant difference in gene expression between patients and controls. However, it has to be emphasized that these patients were diagnosed at a very early stage of kidney disease, that is, they had a short duration of disease before biopsy (mean: 7 months), a near-to-normal serum creatinine and a low level of tubulointerstitial fibrosis (median <10%). Another point potentially

having an impact on the results of this study is the age difference between patients and controls. It has been suggested recently that tissue specific gene expression may alter with age.⁴⁵ Finally, the biopsy provides information on only a specific time point. As renal function was close to normal we cannot draw a conclusion about the changes, which have to occur to alter the balance in favor of disease progression.

Nonetheless, our results underscore the importance of using a genome-wide approach to dissect complex pathophysiological responses during a disease process as focusing on specific pathogenetic pathways does not allow taking into account endogenous counter-regulatory networks. Our study shows that the latter are able at least in some patients to lead to a clinically stable condition. New therapeutic interventions should therefore not only focus on the blockade of deleterious pathways but also might be successful if they increase the self-repair potential.

MATERIALS AND METHODS

Patient characteristics

We used surplus biopsy material stored at -80°C from 19 patients with proteinuria for this study: focal-segmental glomerulosclerosis, $n=6$; minimal-change disease $n=5$; immunoglobulin A nephropathy $n=8$. Biopsies from the unaffected part of kidneys removed because of renal cell carcinoma were used as controls ($n=5$). Light microscopy was performed using hematoxylin/eosin and periodic-acid-Schiff or Pearse-stained sections. A semiquantitative scoring of tubulointerstitial fibrosis was performed by an independent pathologist. Clinical data of patients and controls are shown in Table 2. As renal cell carcinoma is more a disease of the elderly, age was significantly different between patients and controls as was proteinuria. Serum creatinine was normal in the control group and only slightly but not significantly higher in the patient group. The median degree of tubulointerstitial fibrosis was $<10\%$. The study was approved by the institutional review board of the Medical University of Innsbruck.

Isolation of tubule cells from biopsies

After alkaline phosphatase (4-Nitro Blue Tetrazolium Chloride/5-Bromo-4-chloro-3-indolyl phosphate) staining under RNase-free conditions proximal tubular epithelial cells were identified and isolated using the PixCell II[®] Laser Capture Microdissection System and CapSure[™] LCM Caps (Arcturus, Mountain View, CA, USA; Figure 4). Neither the staining nor the LCM procedure affected the quality of the RNA as assessed by agarose gel-electrophoresis and semiquantitative reverse transcription-PCR of beta-actin (data not shown).

RNA isolation, quality control, and linear amplification

Total RNA was isolated using the Pico Pure[™] RNA Isolation Kit (Arcturus, Mountain View, CA, USA). A semiquantitative reverse transcription-PCR of beta-2-microglobulin was carried out and only samples with a positive signal were studied further. Owing to approximately 1 ng of RNA per sample we performed two rounds of linear RNA amplification using the RiboAmp[™] RNA Amplification Kit (Arcturus, Mountain View, CA, USA). The reproducibility and reliability of T7-based linear amplification in the setting of Cy5/Cy3-cDNA microarrays was shown by our group previously.⁴⁶ Amplified Universal Human Reference RNA (Stratagene, La Jolla, CA, USA) served as reference material. The quality of the amplified RNA was assessed by spectrophotometry ($A_{260/280}$), on an ethidium bromide stained 1.5% agarose gel and with the Agilent Bioanalyzer and RNA6000 LabChip[™] Kit (Agilent, Palo Alto, CA, USA). After two rounds of amplification the length of the amplified RNA was 133–1025 bp (Table S4).

Labelling and microarray hybridization

Using the CyScribe cDNA Post-Labeling Kit (Amersham Biosciences, GE Healthcare, UK) 1 μg of amplified sample RNA (Cy5, red) and the reference RNA (Cy3 green) were labelled as described previously.⁴⁶ cDNA microarrays were obtained from Stanford Functional Genomics Facility (www.microarray.org/sfgf/). They contained 41 792 spots representing 30325 genes assigned to a UniGene cluster and 11 467 ESTs. All samples were processed in technical duplicates. Arrays were scanned using a GenePix 4000B microarray scanner and the images were analyzed with the GenePix Pro 4.0 software (Axon Instruments, Union City, CA, USA). The raw data as well as array images were transferred to the Stanford

Table 2 | Characteristics of patients and controls

Clinical	Controls	Patients	P^a
Age (years)	67.6 \pm 8.0	40.8 \pm 16.0	0.0062
Female/male	2/3	6/13	0.2578
S_{crea} (mg/dl)	1.09 \pm 0.10	1.37 \pm 0.89	1.0000
U_{prot} (g/d)	Neg ^a	6.8 \pm 9.7	
Histology			
Degree of tubular atrophy and interstitial fibrosis ^b		Number of patients	
0		2	
1		8	
2		2	
3		4	
4 and 5		0	
Median		1 (i.e. $<10\%$)	

^a P -value was calculated using Mann-Whitney U -test (S_{crea} , age) and two-way-ANOVA (sex). Absence of proteinuria in healthy control subjects was defined as a negative urine dipstick.

^bThe degree of tubulointerstitial fibrosis was examined on PAS- or Pearse-stained material: 0=no fibrosis, 1= $<10\%$, 2=10 to 25%, 3=25 to 50%, 4=50 to 75% and 5= $>75\%$. S_{crea} serum creatinin, U_{prot} urinary protein excretion.

Microarray Database for data storage and advanced data analysis (<http://genome-www5.stanford.edu/MicroArray/SMD>). All experiments were performed according to the minimum information about a microarray experiment microarray guidelines.⁴⁷

Validation of microarray results by real-time PCR

Only approximately 1 ng of total RNA could be isolated from each frozen section. Enough frozen sections were available from seven patient samples included in the analysis (three focal segmental glomerular sclerosis, three immunoglobulin A nephropathy, and one minimal change disease) and from all five controls to allow another RPTEC isolation procedure, and the RNA obtained was pooled. Equal amounts of total RNA isolated from patient biopsies and from control samples were reverse transcribed (Sensiscript RT Kit, Qiagen, Hilden, Germany) according to the manufacturers protocol and used for real-time PCR. We used GAPDH as endogenous control. We selected five genes from five different functional groups (Figure 1): DEFB1 (immune response), TIMP1 (protein modification), DUSP5 (signal transduction), BMP7 (cell differentiation) and RAB4A (intracellular transport). Real-time experiments were performed using Assays-on-Demand™ Gene Expression pre-developed primers and FAM™ labelled TaqMan™ probes (www.allgenes.com; DEFB1 Hs00174765m1; TIMP1 Hs00171558m1; DUSP5 Hs00244839m1; RAB4A Hs00190157m1; BMP7 Hs00233476m1; glyceraldehyde-3-phosphate dehydrogenase Hs99999905m1). Quantification of gene expression was performed on a TaqMan ABI Prism 7700 Sequence Detection System™ using the manufacturer's software (both Applied Biosystems, Foster City, CA, USA).

Data processing, statistical analysis, and functional annotation

After excluding spots with an intensity of <1.2 above background and applying an 80% filter (i.e. accepting only genes with values in at least 80% of the arrays) 24961 features were left for further analysis. Duplicate arrays were combined and the values were averaged. Supervised analysis

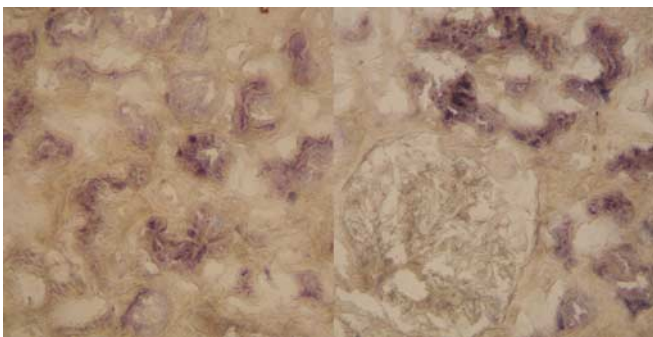


Figure 4 | Staining for alkaline phosphatase to identify proximal tubule cells. Original magnification $\times 40$: after staining for alkaline phosphatase using 4-nitro blue tetrazolium chloride/5-bromo-4-chloro-3-indolyl phosphate (NBT/BCIP), the proximal tubule cells were identified by showing a strong dark blue staining.

combined two statistical procedures to identify differentially expressed genes between patients and controls: significance analysis of microarrays⁴⁸ as well as an unpaired *t*-statistic with correction for multiple testing according to Westfall and Young.⁴⁹ A false discovery rate of <1% was allowed in the significance analysis of microarrays method and only genes showing an adjusted $P < 0.05$ were considered further after *t*-testing.

The genes were further analyzed with regard to their molecular functions and biological processes (Tables S2 and S3) using gene ontology terms from the Gene Ontology Consortium⁵⁰ provided by the SOURCE tool from the Stanford Genomics Facility⁵¹ and the PANTHER classification system.⁵² Biological processes of genes were compared to the PANTHER reference data set. The ratio of expected to the observed frequencies of genes assigned to certain ontology categories were compared by using the χ^2 test to derive significance of differences. Additional functional grouping of genes (as used in Table 1) was based on gene ontology terms and information derived from Pubmed and iHOP.⁵³

Immunohistochemistry

Frozen tissue samples of representative patients and controls were fixed with cold acetone. For antibody dilutions and sources see Table 3. The sections were incubated with the primary antibody for 30 min at room temperature (TSP-3) or overnight at 4°C (BMP-7). For visualization of TSP-3 the mouse ABC Staining System (Santa Cruz Biotechnology, Santa Cruz, CA, USA, www.scbt.com) was used in combination with diaminobenzidine. BMP-7 was detected by the Vectastain Elite ABC Kit (Vector Laboratories, Burlingame, CA, USA, www.vectorlabs.com) and stained with 3-amino-9-ethylcarbazole. Both systems use biotin-conjugated secondary antibodies, avidin and biotinylated horseradish peroxidase and the corresponding chromogen. All sections were counterstained with 3,3'-diaminobenzidine tetrahydrochloride 3-amino-9-ethyl carbazole.

ACKNOWLEDGMENTS

This study was supported by the Fonds zur Förderung der wissenschaftlichen Forschung (FWF) (Grant number P-15678 to GM) and by the National Institutes of Health (Grant number RO1 DK52841 to TWM). We are grateful to the Urology Clinic at the Medical University Innsbruck (Prof. Georg Bartsch) for providing LCM. We appreciate the kind assistance of Kathrin Hochegger and Rita Sarközi during the immunohistochemistry studies. We are also grateful to Herbert Schramek for fruitful discussions during the preparation of this paper. We kindly thank Paul König and Karl Lhotta for establishing the renal biopsy repository, and we also thank Dorothea Heinger for diagnostic evaluation of the kidney biopsies.

SUPPLEMENTARY MATERIAL

Table S1. 62 sequences differentially regulated between patients and controls (open-reading frames, expressed sequence tags and hypothetical proteins).

Table S2. Enriched PANTHER ontology categories, which are significantly upregulated in proteinuric patients.

Table S3. Enriched PANTHER ontology categories, which are significantly downregulated in proteinuric patients.

Table S4. Length of amplified RNA as analyzed on Agilent Bioanalyzer™.

Table 3 | Primary antibodies used for immunohistochemistry

Antigen	Species	Dilution	Source
BMP-7 (N-19)	Goat polyclonal	1:50	Santa Cruz Biotechnologies (www.scbt.com)
TSP-3 (A-12)	Mouse monoclonal	1:500	Santa Cruz Biotechnologies (www.scbt.com)

BMP, bone morphogenetic protein; TSP, thrombospondin.

REFERENCES

1. Coresh J, Astor BC, Greene T *et al.* Prevalence of chronic kidney disease and decreased kidney function in the adult US population: Third National Health and Nutrition Examination Survey. *Am J Kidney Dis* 2003; **41**: 1–12.
2. Garg AX, Mamdani M, Juurlink DN, van WC. Identifying individuals with a reduced GFR using ambulatory laboratory database surveillance. *J Am Soc Nephrol* 2005; **16**: 1433–1439.
3. Tang S, Leung JC, Abe K *et al.* Albumin stimulates interleukin-8 expression in proximal tubular epithelial cells *in vitro* and *in vivo*. *J Clin Invest* 2003; **111**: 515–527.
4. Wang Y, Rangan GK, Tay YC *et al.* Induction of monocyte chemoattractant protein-1 by albumin is mediated by nuclear factor kappaB in proximal tubule cells. *J Am Soc Nephrol* 1999; **10**: 1204–1213.
5. Kitagawa K, Wada T, Furuichi K *et al.* Blockade of CCR2 ameliorates progressive fibrosis in kidney. *Am J Pathol* 2004; **165**: 237–246.
6. Zoja C, Morigi M, Figliuzzi M *et al.* Proximal tubular cell synthesis and secretion of endothelin-1 on challenge with albumin and other proteins. *Am J Kidney Dis* 1995; **26**: 934–941.
7. Zoja C, Donadelli R, Colleoni S *et al.* Protein overload stimulates RANTES production by proximal tubular cells depending on NF-kappa B activation. *Kidney Int* 1998; **53**: 1608–1615.
8. Yard BA, Chorianopoulos E, Herr D, van der Woude FJ. Regulation of endothelin-1 and transforming growth factor-beta1 production in cultured proximal tubular cells by albumin and heparan sulphate glycosaminoglycans. *Nephrol Dial Transplant* 2001; **16**: 1769–1775.
9. Oldroyd SD, Miyamoto Y, Moir A *et al.* An IGF-1 antagonist does not inhibit renal fibrosis in the rat following subtotal nephrectomy. *Am J Physiol Renal Physiol* 2006; **290**: F695–F702.
10. Zeisberg M, Kalluri R. The role of epithelial-to-mesenchymal transition in renal fibrosis. *J Mol Med* 2004; **82**: 175–181.
11. Zeisberg M, Hanai J, Sugimoto H *et al.* BMP-7 counteracts TGF-beta1-induced epithelial-to-mesenchymal transition and reverses chronic renal injury. *Nat Med* 2003; **9**: 964–968.
12. Gollub J, Ball CA, Binkley G *et al.* The Stanford Microarray Database: data access and quality assessment tools. *Nucleic Acids Res* 2003; **31**: 94–96.
13. Qabar A, Derick L, Lawler J, Dixit V. Thrombospondin 3 is a pentameric molecule held together by interchain disulfide linkage involving two cysteine residues. *J Biol Chem* 1995; **270**: 12725–12729.
14. Ziehr J, Sheibani N, Sorenson CM. Alterations in cell-adhesive and migratory properties of proximal tubule and collecting duct cells from bcl-2 $-/-$ mice. *Am J Physiol Renal Physiol* 2004; **287**: F1154–F1163.
15. Yang J, Zhang X, Li Y, Liu Y. Downregulation of Smad transcriptional corepressors SnoN and Ski in the fibrotic kidney: an amplification mechanism for TGF-beta1 signaling. *J Am Soc Nephrol* 2003; **14**: 3167–3177.
16. Todorovic V, Chen CC, Hay N, Lau LF. The matrix protein CCN1 (CYR61) induces apoptosis in fibroblasts. *J Cell Biol* 2005; **171**: 559–568.
17. Ashman N, Harwood SM, Kieswich J *et al.* Albumin stimulates cell growth, l-arginine transport, and metabolism to polyamines in human proximal tubular cells. *Kidney Int* 2005; **67**: 1878–1889.
18. Dixon R, Brunskill NJ. Activation of mitogenic pathways by albumin in kidney proximal tubule epithelial cells: implications for the pathophysiology of proteinuric states. *J Am Soc Nephrol* 1999; **10**: 1487–1497.
19. Erkan E, Devarajan P, Schwartz GJ. Apoptotic response to albumin overload: proximal vs. distal/collecting tubule cells. *Am J Nephrol* 2005; **25**: 121–131.
20. Radtke KP, Fernandez JA, Greengard JS *et al.* Protein C inhibitor is expressed in tubular cells of human kidney. *J Clin Invest* 1994; **94**: 2117–2124.
21. Palmieri D, Lee JW, Juliano RL, Church FC. Plasminogen activator inhibitor-1 and -3 increase cell adhesion and motility of MDA-MB-435 breast cancer cells. *J Biol Chem* 2002; **277**: 40950–40957.
22. Esposito C, Parrilla B, De MA *et al.* Hepatocyte growth factor (HGF) modulates matrix turnover in human glomeruli. *Kidney Int* 2005; **67**: 2143–2150.
23. Ortiz PA, Hong NJ, Garvin JL. Luminal flow induces eNOS activation and translocation in the rat thick ascending limb. *Am J Physiol Renal Physiol* 2004; **287**: F274–F280.
24. Wang T. Role of iNOS and eNOS in modulating proximal tubule transport and acid-base balance. *Am J Physiol Renal Physiol* 2002; **283**: F658–F662.
25. Dedio J, Konig P, Wohlfart P *et al.* NOSIP, a novel modulator of endothelial nitric oxide synthase activity. *FASEB J* 2001; **15**: 79–89.
26. Droin NM, Pinkoski MJ, Dejardin E, Green DR. Egr family members regulate nonlymphoid expression of Fas ligand TRAIL, and tumor necrosis factor during immune responses. *Mol Cell Biol* 2003; **23**: 7638–7647.
27. Dixon R, Brunskill NJ. Albumin stimulates p44/p42 extracellular-signal-regulated mitogen-activated protein kinase in opossum kidney proximal tubular cells. *Clin Sci (London)* 2000; **98**: 295–301.
28. Takaya K, Koya D, Isono M *et al.* Involvement of ERK pathway in albumin-induced MCP-1 expression in mouse proximal tubular cells. *Am J Physiol Renal Physiol* 2003; **284**: F1037–F1045.
29. Senthil D, Choudhury GG, Abboud HE *et al.* Regulation of protein synthesis by IGF-I in proximal tubular epithelial cells. *Am J Physiol Renal Physiol* 2002; **283**: F1226–F1236.
30. Iglesias J, Levine JS. Albuminuria and renal injury – beware of proteins bearing gifts. *Nephrol Dial Transplant* 2001; **16**: 215–218.
31. Arici M, Chana R, Lewington A *et al.* Stimulation of proximal tubular cell apoptosis by albumin-bound fatty acids mediated by peroxisome proliferator activated receptor-gamma. *J Am Soc Nephrol* 2003; **14**: 17–27.
32. Erkan E, Garcia CD, Patterson LT *et al.* Induction of renal tubular cell apoptosis in focal segmental glomerulosclerosis: roles of proteinuria and Fas-dependent pathways. *J Am Soc Nephrol* 2005; **16**: 398–407.
33. Iglesias J, Abernethy VE, Wang Z *et al.* Albumin is a major serum survival factor for renal tubular cells and macrophages through scavenging of ROS. *Am J Physiol* 1999; **277**: F711–F722.
34. Border WA, Noble NA. Transforming growth factor beta in tissue fibrosis. *N Engl J Med* 1994; **331**: 1286–1292.
35. Sporn MB. The importance of context in cytokine action. *Kidney Int* 1997; **51**: 1352–1354.
36. Hruska KA, Guo G, Wozniak M *et al.* Osteogenic protein-1 prevents renal fibrogenesis associated with ureteral obstruction. *Am J Physiol Renal Physiol* 2000; **279**: F130–F143.
37. Vukicevic S, Basic V, Rogic D *et al.* Osteogenic protein-1 (bone morphogenetic protein-7) reduces severity of injury after ischemic acute renal failure in rat. *J Clin Invest* 1998; **102**: 202–214.
38. Wang S, Chen Q, Simon TC *et al.* Bone morphogenetic protein-7 (BMP-7), a novel therapy for diabetic nephropathy. *Kidney Int* 2003; **63**: 2037–2049.
39. Zeisberg M, Bottiglio C, Kumar N *et al.* Bone morphogenetic protein-7 inhibits progression of chronic renal fibrosis associated with two genetic mouse models. *Am J Physiol Renal Physiol* 2003; **285**: F1060–F1067.
40. Zeisberg M, Shah AA, Kalluri R. Bone morphogenetic protein-7 induces mesenchymal to epithelial transition in adult renal fibroblasts and facilitates regeneration of injured kidney. *J Biol Chem* 2005; **280**: 8094–8100.
41. Terada Y, Tanaka H, Okado T *et al.* Expression and function of the developmental gene Wnt-4 during experimental acute renal failure in rats. *J Am Soc Nephrol* 2003; **14**: 1223–1233.
42. Surendran K, Schiavi S, Hruska KA. Wnt-dependent beta-catenin signaling is activated after unilateral ureteral obstruction, and recombinant secreted frizzled-related protein 4 alters the progression of renal fibrosis. *J Am Soc Nephrol* 2005; **16**: 2373–2384.
43. Nelson WJ, Nusse R. Convergence of Wnt, beta-catenin, and cadherin pathways. *Science* 2004; **303**: 1483–1487.
44. Hellberg CB, Burden-Gulley SM, Pietz GE, Brady-Kalnay SM. Expression of the receptor protein-tyrosine phosphatase PTPmu, restores E-cadherin-dependent adhesion in human prostate carcinoma cells. *J Biol Chem* 2002; **277**: 11165–11173.
45. Melk A, Mansfield ES, Hsieh SC *et al.* Transcriptional analysis of the molecular basis of human kidney aging using cDNA microarray profiling. *Kidney Int* 2005; **68**: 2667–2679.
46. Rudnicki M, Eder S, Schratzberger G *et al.* Reliability of t7-based mRNA linear amplification validated by gene expression analysis of human kidney cells using cDNA microarrays. *Nephron Exp Nephrol* 2004; **97**: e86–e95.
47. Brazma A, Hingamp P, Quackenbush J *et al.* Minimum information about a microarray experiment (MIAME)-toward standards for microarray data. *Nat Genet* 2001; **29**: 365–371.
48. Tusher VG, Tibshirani R, Chu G. Significance analysis of microarrays applied to the ionizing radiation response. *Proc Natl Acad Sci USA* 2001; **98**: 5116–5121.
49. Westfall PH, Young SS. *Resampling-based Multiple Testing: Examples and Methods for P-Value Adjustment*. Wiley Series in Probability and Mathematical Statistics. Wiley: New York, 1993.
50. Ashburner M, Ball CA, Blake JA *et al.* Gene ontology: tool for the unification of biology. The Gene Ontology Consortium. *Nat Genet* 2000; **25**: 25–29.
51. Diehn M, Sherlock G, Binkley G *et al.* SOURCE: a unified genomic resource of functional annotations, ontologies, and gene expression data. *Nucleic Acids Res* 2003; **31**: 219–223.
52. Thomas PD, Kejariwal A, Campbell MJ *et al.* PANTHER: a browsable database of gene products organized by biological function, using curated protein family and subfamily classification. *Nucleic Acids Res* 2003; **31**: 334–341.
53. Hoffmann R, Valencia A. A gene network for navigating the literature. *Nat Genet* 2004; **36**: 664.